Journal of the European Ceramic Society 22 (2002) 447–452
www.elsevier.com/locate/jeurceramsoc

Damage assessment of alumina fibre-reinforced mullite ceramic matrix composites subjected to cyclic fatigue at ambient and elevated temperatures

C. Kaya[a,b,*], F. Kaya[a,b], H. Mori[c,1]

[a]IRC in Materials for High Performance Applications, The University of Birmingham, Edgbaston, Birmingham B15 2TT, UK
[b]School of Metallurgy and Materials, The University of Birmingham, Edgbaston, Birmingham B15 2TT, UK
[c]Research Centre for Advanced Science and Technology (RCAST), The University of Tokyo, Tokyo, Japan

Received 3 February 2001; received in revised form 4 April 2001; accepted 25 April 2001

Abstract

The damage evaluation behaviour of alumina fibre-reinforced mullite ceramic matrix composites subjected to cyclic fatigue was investigated by means of acoustic emission (AE) monitoring and forced resonance techniques. AE technique provided sufficient information about the damage initiation and progression in real time whilst the forced resonance (FR) technique allowed the detection of changes in elastic modulus (E) and internal friction (Q^{-1}) that occurred with increasing number of cyclic fatigue at room temperature. From the two non-destructive detection techniques results combined with microstructural observations, it is concluded that the composite cyclic fatigue damage evolution begins with multiple crack formation within the matrix and is followed by delamination (interfacial failure). Final failure of the composite is caused by fibre fracture and extensive cyclic sliding along the fibre/matrix interface. The strong bonding between mullite matrix and alumina fibre caused by the glassy phase within the mullite matrix determined the fatigue performance of the composite at 1350°C. Regions with glassy phase failed catastrophically as a result of early fibre fracture.

Keywords: Acoustic emission; Al_2O_3-fibres; Composites; Damage assessment; Fatigue; Internal friction; Mullite

1. Introduction

Mullite ($3Al_2O_3{\cdot}2SiO_2$) and its composites reinforced with either fibres or particulates are prime candidate materials for use in advanced structural and high temperature applications, because of their good thermal shock and creep resistance, excellent chemical and thermal stability, low thermal expansion and conductivity and moderate fracture toughness.[1]

In service, fibre-reinforced CMCs will be subject to tensile, flexural or compressive creep and cyclic fatigue loading (gas turbine airfoils/rotors, heat exchanger, vanes and combustors) in a high temperature oxidasing environment. Thus, a better understanding of cyclic fatigue behaviour and damage mechanisms occur during cyclic fatigue loading of fibre-reinforced composites is an essential requirement for long-term structural reliability and accurate life-prediction procedure, as well as reliable structural design at room and high temperature.[2–10]

When a fibre-reinforced composite is subjected to a cyclic fatigue loading, a variety of damage mechanisms, such as matrix microcracking, fibre-matrix debonding, interfacial failure or delamination and fibre fracture can take place. As the damage progresses in composite, energy is released in different forms, such as acoustic waves. The energy or the amplitude of the acoustic waves depends on type of fracture event which can be detected by monitoring the AE. Each fracture event, such as delamination or fibre fracture can easily be separated and determined by analysing AE parameters, including amplitude, duration, time, number of event, energy, etc.[11–14]

The objective of this investigation is to asses the damage mechanisms of the Saffil alumina fibre-reinforced mullite CMCs under cyclic fatigue at room

* Corresponding author. Tel.: +44−121-4143537; fax: +44−121-4143441.
E-mail address: c.kaya@bham.ac.uk (C. Kaya).
1 Present address: Railway Technical Research Institute, Materials Engineering Division, Kokubunji-Shi, Tokyo, 185-8540, Japan.

0955-2219/02/$ - see front matter
PII: S0955-2219(01)00320-X

temperature and 1350°C. The state-of-damage caused by cyclic fatigue was characterised using FR and AE monitoring, as non-destructive tests. The first one involves dynamic measurement of the Young's modulus (E) and the internal friction (Q^{-1}) of the specimen subjected to cyclic fatigue. AE analyses were performed during room temperature cyclic fatigue to establish the damage initiation and progression in real time.

2. Experimental procedure

2.1. Fatigue tests at ambient and elevated temperature

The room and elevated (1350°C) temperature cyclic fatigue behaviour of an alumina fibre-reinforced mullite ceramic matrix composite has been studied. The details of the manufacturing techniques of the composites (contain 30 vol.% multidirectional fibres) tested here are presented elsewhere.[15–18] The tests were performed using an Instron 8500 testing machine fitted with a Instron 6761R high temperature, turbomolecular pump vacuum furnace. During the high temperature tests, a vacuum of the order of 133×10^{-6} Pa was obtained. All tests were carried out on unnotched specimens ($45\times5\times3.5$ mm^3) using a four-point bending (outer span is 40 mm and inner span is 20 mm). The stress ratio, R, ($\sigma_{min}/\sigma_{max}$) and loading frequency values were kept constant at 0.5 and 10 Hz, respectively. During the room temperature fatigue tests, some tests were interrupted periodically (after every 2×10^5 cycles) to remove the specimen in order to measure its Young's modulus and internal friction using a forced resonance technique. Fatigue life diagrams (S–N curve) were plotted also using different stress levels to identify the composite performance at room temperature and 1350°C. The damage accumulation due to room temperature cyclic fatigue was monitored using acoustic emission (AE) technique (see Fig. 1), while the cyclic fatigue failure mechanisms at room and high temperature were analysed on a microstructural level using transmission electron microscopy (TEM, Philips CM 20 and Jeol 4000-FX) and high resolution scanning electron microscopy (Hitachi S-4000, Field Emission Gun, FEG SEM).

2.2. Young's modulus (E) and internal friction (Q^{-1}) measurements by forced resonance technique

The forced resonance system measures the Young's modulus and the internal friction of a material by use of the free-free resonant beam method.[19,20] This is a non-destructive test, and can be used to assess damage within a material which otherwise would not be detectable without destroying the sample. The basic electrical set-up of the apparatus used is shown in Fig. 2. A sine wave signal is sent to the driver, via a switching circuit and an audio amplifier. The output of the cartridge is amplified and filtered to remove the low frequency component and reduce noise. The resulting signal is measured on the ac voltmeter and analysed using the PC oscilloscope software. For Young's modulus measurements, the resonant frequency of the sample is measured using the frequency counter and the a.c. voltmeter. For the resonant frequency to be within the measurable range of 1–10 kHz, the sample dimensions and mass should be chosen carefully. The mass must be less than 12 g, as the specimen has to be supported from a delicate stylus. However, the mass should not be less than 3 g, as sample coupling problems may occur. The length to width ratio and the length to thickness ratio should both be greater than 3:1.[21] The specimen surface should be flat and parallel to within ±0.002 mm. The mass of the sample should be measured to ±0.001 g. Comprehensive information about the technique and equation used to calculate E and Q^{-1} can be found in the literature.[22,23]

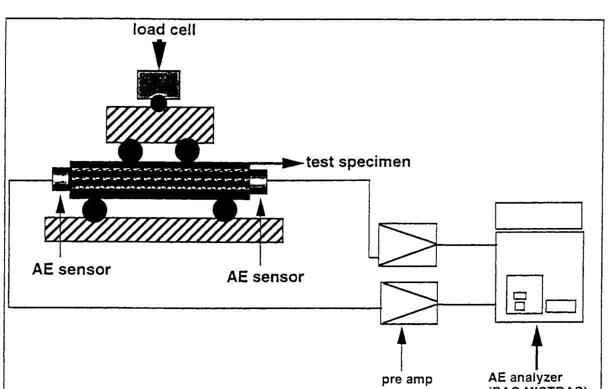

Fig. 1. Schematic representation of 4-point bending cyclic fatigue test arrangement and AE monitoring system, showing the location of the high sensitive sensors.

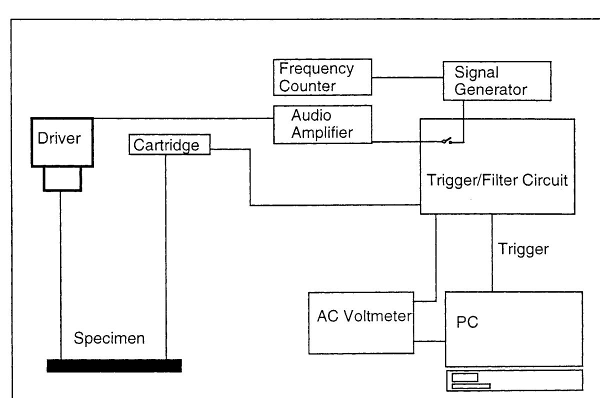

Fig. 2. Schematic diagram of the electrical set-up of the measuring apparatus used for determining the Young's modulus and internal friction using forced resonance technique.

3. Results and discussion

Fig. 3 is a plot of the nominal maximum stress, σ_{max} applied in 4-point bending cyclic fatigue against the number of cycles to failure (so called the fatigue life diagram or S–N curve), at room temperature and 1350°C, for Saffil alumina fibre-reinforced (30 vol.%) mullite CMCs under a stress ratio ($\sigma_{min}/\sigma_{max}$) of 0.5 and a loading frequency of 10 Hz. No fatigue failure was observed up to 1.5×10^6 cycles when the maximum stress, σ_{max} was 357 MPa, which is 70% of the 4-point bending strength of this composite at room temperature, or less. The graph shows that for σ_{max} above 357 MPa, the number of cycles to failure decreased as σ_{max} increased, although this composite material survived up to 6.5×10^5 cycles under a σ_{max} level of 375 MPa. At 1350°C, no fatigue failure of the composite was observed up to 1×10^6 cycles when the maximum stress, σ_{max} was 280 MPa, which is 70% of the 4-point bending strength of this composite at this temperature, or less. In this case, the number of cycles to failure decreased as σ_{max} increased above 280 MPa, although this composite material survived up to 6×10^5 cycles under a σ_{max} level of 300 MPa.

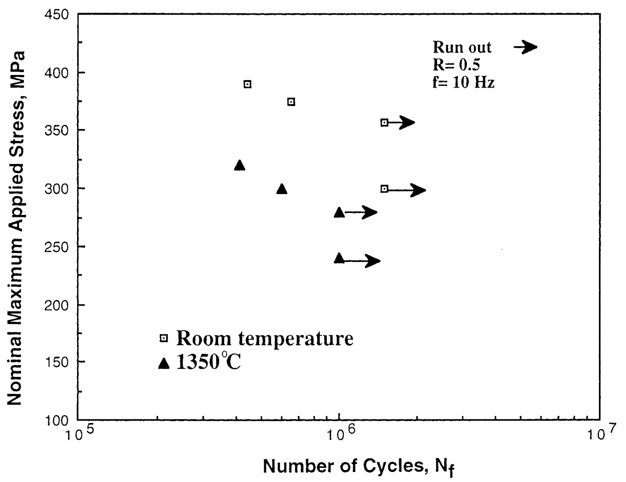

Fig. 3. Nominal maximum stress, σ_{max} applied in 4-point bending cyclic fatigue versus the number of cycles to failure (the so-called S–N curve or fatigue life diagram) for Saffil alumina fibre-reinforced (30 vol.%) mullite CMCs at room temperature and 1350°C, under a stress ratio ($\sigma_{min}/\sigma_{max}$) of 0.5 and a loading frequency of 10 Hz.

The AE results corresponding to the development of different composite microstructural damage mechanisms are shown in Fig. 4. Acoustic emissions were recorded and classified into three stages based on the energy level of the acoustic events, noting that Saffil alumina fibres have a higher Young's modulus (300 GPa) than the mullite matrix (200–220 GPa). Acoustic events having an energy level higher than 95 μJ were accepted as fibre fracture, as shown in the top section of the graph. Events having an energy level between 60 and 95 μJ were attributed to matrix cracking (middle section). Saffil alumina fibre-reinforced mullite CMCs tested here exhibit very low interfacial bonding or no bonding or contact at all in places;[15] consequently, acoustic emissions at an energy level below 60 μJ were taken as indicative of interfacial failure (delamination) as shown in the bottom section of the graph.

The effect of cyclic fatigue at room temperature with $\sigma_{max} = 332$ MPa (i.e. 65% of the 4-point bending strength of this composite at this temperature) on the

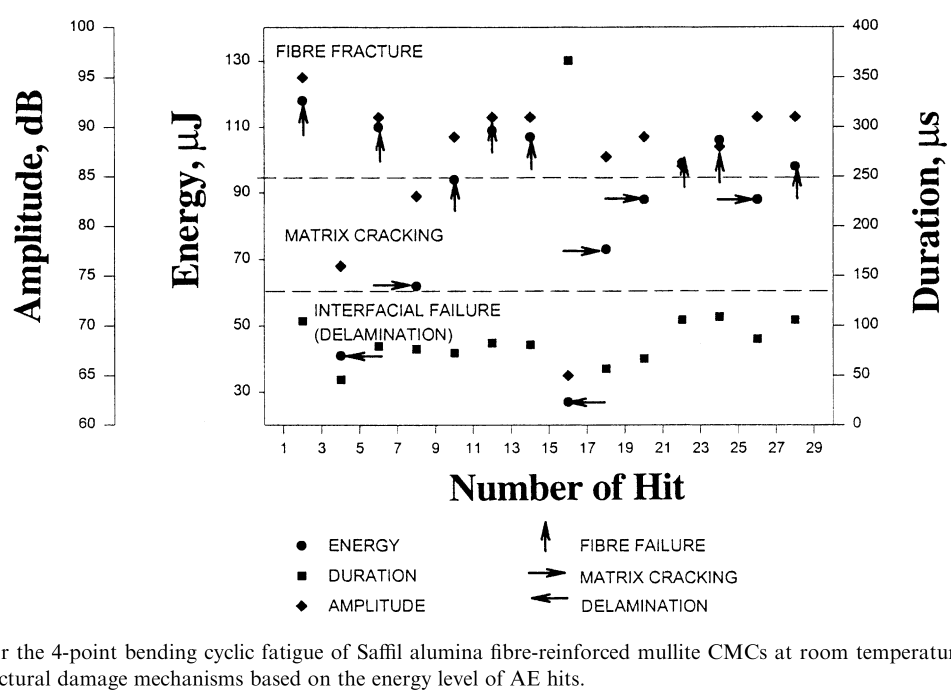

Fig. 4. AE events for the 4-point bending cyclic fatigue of Saffil alumina fibre-reinforced mullite CMCs at room temperature, showing the development of microstructural damage mechanisms based on the energy level of AE hits.

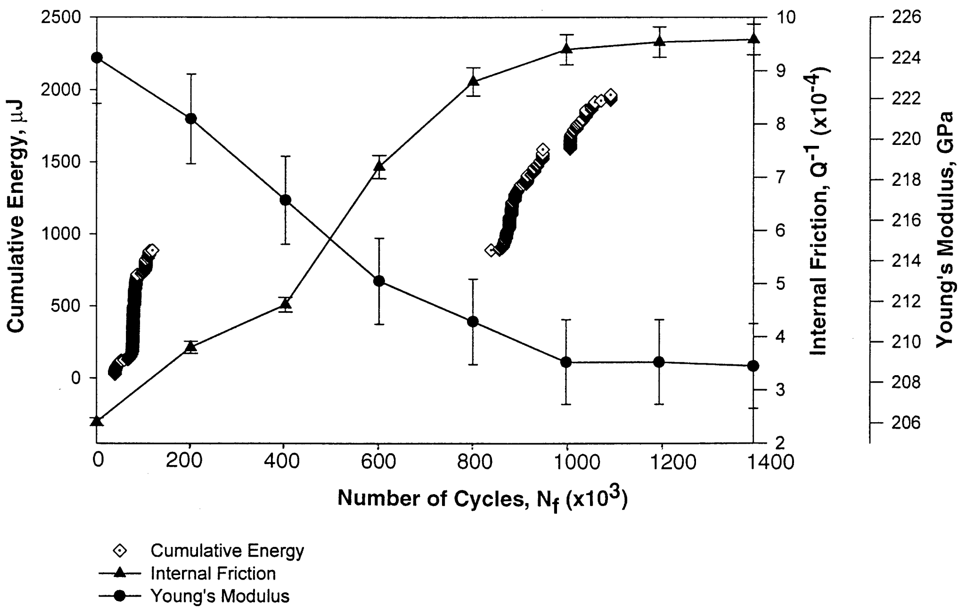

Fig. 5. The effect of 4-point bend cyclic fatigue at room temperature with $\sigma_{max} = 332$ MPa on the Young's modulus (E) and internal friction (Q^{-1}) and AE cumulative event energy of the Saffil alumina fibre-reinforced mullite CMCs.

Young's modulus (E) and internal friction (Q^{-1}) of Saffil alumina fibre-reinforced mullite CMCs is shown in Fig. 5. After 1.4×10^6 cycles, the Young's modulus had decreased by 7%, whereas the internal friction had increased by 350%, indicating the higher sensitivity of Q^{-1} to microstructural damage. After each period of 2×10^5 cycles, E decreased by 1.1%, whilst Q^{-1} increased by almost 60%. The steady decrease in E was attributed to progressive interfacial debonding and microcrack generation as the number of cycles is increased. The sharp increase in Q^{-1} after 4×10^5 cycles is evidence for the onset of more extensive microstructural damage, such as matrix microcracking and fibre/matrix delamination, resulting in the creation of new internal surfaces within the composite. The AE parameter considered as a function of the number of fatigue cycles was the cumulative energy of the event. It is seen that acoustic events with a relatively low energy occurred during the early stages of cyclic fatigue (between 50×10^3 and 200×10^3 cycles). These are most likely associated with the onset of matrix microcracking. Note, however, that no AE data were obtained during cyclic fatigue between 2×10^5 and 8×10^5 cycles, because individual event energies were too low to be detectable above the background noise threshold. This suggests that internal friction is a very sensitive parameter for indicating the occurrence of cumulative microstructural damage comprising very low energy individual damage-causing events, such as interfacial failure/delamination. Between 8×10^5 cycles and 1.2×10^6 cycles, AE data were again obtained but at a higher cumulative energy level. These higher energy events represent fibre fracture.

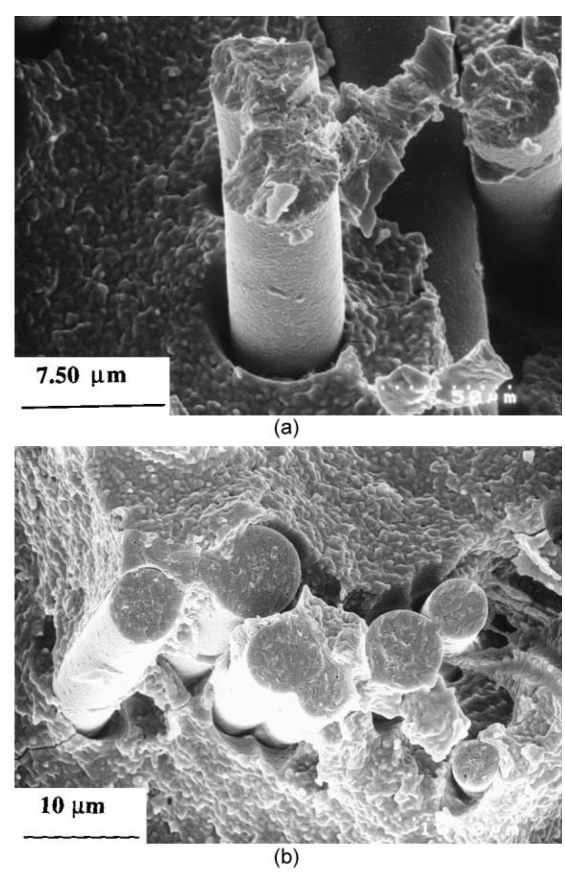

Fig. 6. FEG SEM micrographs of composites subjected to cyclic fatigue until failure, showing (a) less fibre/matrix bonding and/or greater fibre pull-out after 4.4×10^5 cycles at room temperature with $\sigma_{max} =$ 390 MPa and (b) greater fibre/matrix bonding and/or less fibre pull-out after 4.1×10^5 cycles at 1350°C with $\sigma_{max} = 320$ MPa.

Microstructural observations to characterize the cycles fatigue damage evaluation at 1350×C showed that pull-out length of the fibres is shorter than that identified at room temperature, as shown in Fig. 6. This suggests that, at this temperature, there might be a regional interaction or partial reaction between glassy phase within the mullite matrix (presence of this glassy phase in mullite matrix was determined in our previous study)[16] and alumina fibre, leading a partially strong bonding in this particular area, and this might result a fibre failure, as shown in Fig. 6. Fig. 6 shows FEG SEM micrographs of fracture surfaces of samples subjected to cyclic fatigue until failure at (a) room temperature and (b) 1350°C, at a different maximum stress which caused failure after 4×10^5 cycles at both temperatures. Comparing the fracture surfaces indicates that at room temperature there is less fibre/matrix bonding and/or greater fibre pull-out than at 1350°C. This suggests that at 1350°C, there is a local interaction between the glassy phase within the mullite matrix and Saffil alumina fibre, leading to particularly strong bonding in this region resulting in fibre failure.

Fig. 7(a) shows a region where strong bonding between the glassy phase within the mullite and Saffil alumina fibre took place (after 6×10^5 cycles) resulting in fibre fracture in this region. In the absence of any glassy phase or intimate contact between the matrix and fibre, matrix microcracks can be arrested as shown in Fig. 7(b), increasing the number of cycles to failure. As shown in Fig. 3, the specimen tested at 1350°C exhibits a shorter cyclic fatigue life than those tested at room temperature. This behaviour was attributed to the development of strong localised bonding at elevated temperatures, preventing fibre pull-out and resulting in brittle fracture of the composite.[24] FEG SEM observations showed that where the bridging of matrix cracks by fibres occurred, catastrophic failure of the composite at 1350°C was prevented, as shown in Fig. 8(a). This mechanism enhances fatigue resistance at high temperature. However, repeated sliding along the fibre-matrix interface

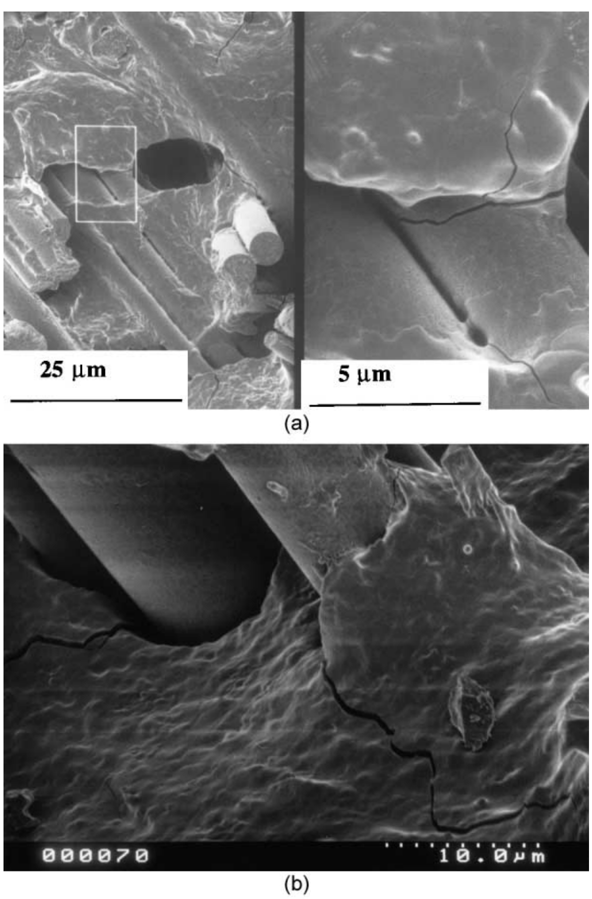

Fig. 7. FEG SEM micrographs of composites subjected to cyclic fatigue at 1350°C (cycles to failure $=6\times10^5$ at $\sigma_{max} = 300$ MPa), showing locally strong bonding between the glassy phase within the mullite matrix and the Saffil alumina fibre, causing (a) fibre failure and (b) the arrest of matrix microcracks, owing to the absence of intimate contact with the Saffil fibre (total cycles to failure is 6×10^5).

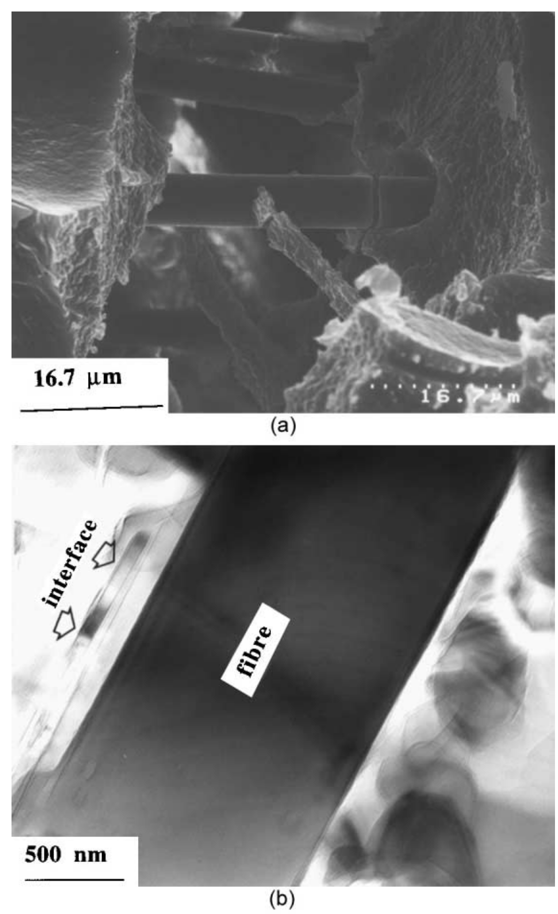

Fig. 8. (a) FEG SEM micrograph, showing fibre-bridging in a sample subjected to cyclic fatigue at 1350°C (after 6×10^5 cycles) and (b) bright field TEM micrograph, showing the extensive damage of the interface between the mullite matrix and the Saffil alumina fibre which occurs at 1350°C.

caused wear in this region, resulting in extensive interface damage, as shown in Fig. 8(b).

4. Conclusion

The state-of-damage in Saffil alumina fibre-reinforced RBM CMCs subjected to cyclic fatigue was investigated by means of acoustic emission (AE) monitoring and dynamic forced resonance (FR) techniques. FR measurements showed that after 10^6 cycles, the Young's modulus decreased by 7%, whereas the internal friction increased by 350%, indicating the higher sensitivity of Q^{-1} to microstructural damage. The sharp increase in Q^{-1} after 4×10^5 cycles is evidence for the development of significant microstructural damage, such as matrix cracking and delamination, resulting in the creation of new internal surfaces within the composite. The TEM and HRSEM results showed that the occurrence of locally strong bonding between the mullite matrix and the Saffil alumina fibre (caused by regions of glassy phase within the mullite matrix) is what determined the fatigue performance of the composite at 1350°C. Regions with a glassy phase failed catastrophically as a result of fibre fracture, whereas the absence of intimate contact between the mullite matrix and the Saffil fibres resulted in crack arrest. A longer fatigue life at room temperature corresponded to less fibre/matrix bonding and/or greater fibre pull-out, while at 1350°C the converse was apparent. According to the AE and FR results plus the microstructural observations, it appears that the composite cyclic fatigue damage evolution begins with multiple crack formation within the matrix and is followed by delamination (interfacial failure). Final failure of the composite most probably occurs by fibre fracture with extensive cyclic sliding along the fibre/matrix interface.

Acknowledgements

Professor M.H. Loretto and I.R. Harris are acknowledged for the provision of laboratory facilities in the IRC and the School of Metallurgy and Materials, respectively.

References

1. Somiya, S., Davis, R. F. and Pask, J. A. (ed.), Mullite and Mullite Matrix Composites. *Ceramics Transactions*, Vol. 6. American Ceramic Society, Westerville, OH.
2. Evans, A. G. and Zok, F. W., The physics and mechanics of fibre-reinforced brittle matrix composites. *J. Mater. Sci.*, 1994, **29**, 3857–3896.
3. Reynaud, P., Rouby, D., Fantozzi, G., Abbe, F. and Peres, P., *High Temperature Ceramic-Matrix Composites I: Design, Durability, and Performance*. The American Ceramic Society, OH, 1995.
4. Reynaud, P., Rouby, D., Fantozzi, G. and Abbe, F. Effects of interfacial evolutions on the mechanical behaviour of ceramic matrix composites during cyclic fatigue. *Scripta Metall.*, 31 1994 1061–1066.
5. Kotil, T., Holmes, J. W. and Comninou, M., Origin of hysteresis observed during fatigue of ceramic-matrix composites. *J. Am. Ceram. Soc.*, 1990, **73**, 1879–1883.
6. Marshall, D. B. and Evans, A. G., Failure mechanisms in ceramic-fiber/ceramic matrix composites. *J. Am. Ceram. Soc.*, 1985, **68**, 225–231.
7. Thouless, M. D. and Evans, A. G., Effects of pull-out on the mechanical properties of ceramic-matrix composites. *Acta Metall.*, 1988, **36**, 517–522.
8. Reynaud, P., Cyclic fatigue of ceramic-matrix composites at ambient and elevated temperatures. *Comp. Sci. Technol.*, 1996, **56**, 809–814.
9. Morris, I. W., Cox, B. N., Marshall, D. B., Inman, R. V. and James, M. R., Fatigue mechanism in graphite/SiC composites at room and high temperature. *J. Am. Ceram. Soc.*, 1994, **77**, 792–800.
10. Rouby, D. and Reynaud, P., Fatigue behaviour related to interface modification during load cycling in ceramic-matrix fibre composites. *Comp. Sci. Technol.*, 1993, **48**, 109–118.
11. Dzenis, Y. A. and Qian, J., Analysis of microdamage evolution histories in composites. *Int. J. Solids Structures*, 2001, **38**(10–13), 1831–1854.
12. Beattie, A. G., Acoustic emission, principles and instrumentation. *Journal of Acoustic Emission*, 1983, **2**(1/2), 95–128.
13. Phoenix, S. L., Statistical issues in the fracture of brittle-matrix fibrous composites. *Comp. Sci. Technol.*, 1993, **48**(1-4), 65–80.
14. Enoki, M, Ohtake, S. and Kishi, T., Classification of microfracture process type in glass matrix composites by quantitative acoustic emission method. *Materials Transactions JIM*, 2001, **42**(1), 108–113.
15. Kaya, C., *Processing and Properties of Alumina Fibre-reinforced Mullite Ceramic Matrix Composites*. PhD thesis, June 1999, The University of Birmingham, UK.
16. Kaya, C., Trusty, P. A. and Ponton, C. B., Electrophoretic filtration deposition (EFD) of Saffil alumina fibre-reinforced mullite multilayer nano-ceramic matrix composites. *Ceram. Trans.*, 1998, **83**, 399–406.
17. Kaya, C., Trusty, P. A. and Ponton, C. B., Preparation of heterocoagulated colloidal suspensions for fabrication of ceramic matrix composites by electrophoretic filtration deposition. *Br. Ceram. Trans.*, 1998, **97**, 48–54.
18. Kaya, C., Trusty, P. A., and Ponton, C. B., Optimisation of nano-size colloidal suspension for fabrication ceramic matrix composites using electrophoretic deposition. In *Proceedings of Better Ceramics Through Processing*, The Institute of Materials, London, UK, 1998, pp. 101–108.
19. Spinner, S. and Tefft, W. E., A method for determining mechanical resonance frequencies and for calculating elastic moduli from these frequencies. *American Society for Testing and Materials Proceeedings*, 1961, **61**, 1221–1238.
20. Spinner, S., Reichard, T. W. and Tefft, W. E., A comparison of experimental and theoretical relations between Young's modulus and flexural and longitudinal resonance frequencies of uniform bars. *J. Research, Nat. Bureau of Standards*, 1960, **64A**, 147–155.
21. Standart test method for Young's modulus, shear modulus, and Poission's ratio for glass and glass-ceramics by resonance. *ASTM Standard*, 1989, C623.
22. Timms, L. A., *The Processing, Microstructure and Properties of Alumina/silicon Carbide Nanocomposites*. PhD thesis, August 1998, The University of Birmingham, UK.
23. Nowick, A. S. and Berry, B. S., *Anelastic Relaxation in Crystalline Solids*. Academic Press, New York, 1972.
24. Nair, V. S. and Jakus, K., *High Temperature Mechanical Behaviour of Ceramic Composites*. Butterworth-Heinemann, Massachusetts, 1995.